

SpecSolve: Spectral methods for spectral measures

Matthew J. Colbrook, Andrew Horning

Abstract Self-adjoint operators on infinite-dimensional spaces with continuous spectra are abundant but do not possess a basis of eigenfunctions. Rather, diagonalization is achieved through spectral measures. The SpecSolve package [SIAM Rev., 63(3) (2021), pp. 489–524] computes spectral measures of general (self-adjoint) differential and integral operators by combining state-of-the-art adaptive spectral methods with an efficient resolvent-based strategy. The algorithm achieves arbitrarily high orders of convergence in terms of a smoothing parameter, allowing computation of both discrete and continuous spectral components. This article extends SpecSolve to two important classes of operators: singular integro-differential operators and general operator pencils. Essential computational steps are performed with off-the-shelf spectral methods, including spectral methods on the real line, the ultraspherical spectral method, Chebyshev and Fourier spectral methods, and the (hp -adaptive and sparse) ultraspherical spectral element method. This collection illustrates the power and flexibility of SpecSolve’s “discretization-oblivious” paradigm.

Key words: spectral measures, spectral methods

2010 Mathematics Subject Classification: 47A10, 46N40, 47N50, 65N35, 81Q10

1 Introduction

Any finite and self-adjoint matrix $A \in \mathbb{C}^{n \times n}$ has an orthonormal basis of eigenfunctions. This basis diagonalizes A by decomposing the space \mathbb{C}^n into a sum of

Matthew J. Colbrook

Department of Applied Mathematics and Theoretical Physics, University of Cambridge, Cambridge, CB3 0WA and Centre Sciences des Données, Ecole Normale Supérieure, 45 rue d’Ulm, 75005 Paris. e-mail: m.colbrook@damtp.cam.ac.uk

Andrew Horning

Department of Mathematics, Massachusetts Institute of Technology, 182 Memorial Dr, Cambridge, MA 02142, United States. e-mail: horninga@mit.edu

orthogonal eigenspaces. However, many applications require us to study a self-adjoint operator \mathcal{L} with domain $\mathcal{D}(\mathcal{L}) \subset \mathcal{H}$ on an *infinite-dimensional* Hilbert space \mathcal{H} with inner product $\langle \cdot, \cdot \rangle$. Even when given a finite matrix A , it is often an approximation or discretization of an underlying infinite-dimensional operator. In infinite dimensions, there may not exist a basis of eigenfunctions since \mathcal{L} can have a continuous spectral component. This situation arises in, for example, stochastic processes and signal-processing [1, 2] [3, Ch. 7], scattering in particle physics [4, 5], density-of-states in materials [6, 7], and many other areas [8–11].

Instead of eigenfunctions, \mathcal{L} can be diagonalized through spectral measures supported on its spectrum $\Lambda(\mathcal{L}) \subset \mathbb{R}$ (see section 2 and eq. (3)). While efficient methods for computing spectral measures of (even very large) finite matrices exist [7], the infinite-dimensional case is more subtle. Most existing methods focus on specific operators where analytical formulas are available or perturbations of such cases [12, Section 3]. Recently, [12] developed methods for computing spectral measures of general ODEs and integral operators using two ingredients:

1. A numerical solver for shifted linear equations $(\mathcal{L} - z)u = f$ for $z \in \mathbb{C} \setminus \Lambda(\mathcal{L})$.
2. Numerical approximations to inner products of the form $\langle u, f \rangle$.

The software `SpecSolve` [13] implements these ingredients using spectral methods.

This article extends `SpecSolve` to two important classes of operators with continuous spectra: singular integro-differential operators and operator pencils. Leveraging sparse spectral methods for the Hilbert transform on the real line, we compute spectral measures of singular integral operators such as

$$[\mathcal{L}u](x) = a(x)u(x) + \frac{1}{\pi i} \int_{\mathbb{R}} \frac{G(x, y)}{y - x} u(y) dy, \quad (1)$$

where $G(x, y) = \overline{G(y, x)}$ and real-valued $a(x)$ satisfy appropriate regularity constraints on \mathbb{R} . Differential terms are straightforward to incorporate to tackle a broad class of singular integro-differential operators. We also extend the two-step framework to compute spectral measures associated with the generalized spectral problem $\mathcal{A}v = \lambda \mathcal{B}v$, for operators \mathcal{A} and \mathcal{B} . The two essential computational steps are performed with off-the-shelf spectral methods, illustrating the power and flexibility of `SpecSolve`'s "discretization-oblivious" paradigm.

2 Spectral measures

The spectral theorem for a finite self-adjoint matrix $A \in \mathbb{C}^{n \times n}$ states that there exists an orthonormal basis of eigenvectors v_1, \dots, v_n for \mathbb{C}^n such that

$$v = \left(\sum_{k=1}^n v_k v_k^* \right) v, \quad v \in \mathbb{C}^n \quad \text{and} \quad Av = \left(\sum_{k=1}^n \lambda_k v_k v_k^* \right) v, \quad v \in \mathbb{C}^n, \quad (2)$$

where $\lambda_1, \dots, \lambda_n$ are eigenvalues of A , i.e., $Av_k = \lambda_k v_k$ for $1 \leq k \leq n$. In other words, the projections $v_k v_k^*$ decompose \mathbb{C}^n and diagonalize A .

Switching to infinite dimensions, associated with the operator \mathcal{L} is a projection-valued measure, \mathcal{E} [14, Theorem VIII.6], whose support is the spectrum $\Lambda(\mathcal{L})$. The measure \mathcal{E} assigns an orthogonal projector to each Borel subset of \mathbb{R} such that

$$f = \left(\int_{\mathbb{R}} d\mathcal{E}(y) \right) f, \quad f \in \mathcal{H} \quad \text{and} \quad \mathcal{L}f = \left(\int_{\mathbb{R}} y d\mathcal{E}(y) \right) f, \quad f \in \mathcal{D}(\mathcal{L}). \quad (3)$$

Here, $\mathcal{D}(\mathcal{L})$ denotes the domain of the operator \mathcal{L} . Analogous to (2), the relations in (3) show how \mathcal{E} decomposes \mathcal{H} and diagonalizes the operator \mathcal{L} .

Of particular interest are the (scalar-valued) spectral measures of \mathcal{L} with respect to $f \in \mathcal{H}$, given by $\mu_f(\Omega) := \langle \mathcal{E}(\Omega)f, f \rangle$, for Borel-measurable sets $\Omega \subset \mathbb{R}$. Lebesgue's decomposition of μ_f is

$$d\mu_f(y) = \underbrace{\sum_{\lambda \in \Lambda^p(\mathcal{L})} \langle \mathcal{P}_\lambda f, f \rangle \delta(y - \lambda) dy}_{\text{discrete part}} + \underbrace{\rho_f(y) dy + d\mu_f^{(\text{sc})}(y)}_{\text{continuous part}}.$$

The discrete part of μ_f is a sum of Dirac delta distributions, supported on the set of eigenvalues of \mathcal{L} , which we denote by $\Lambda^p(\mathcal{L})$. The coefficient of each δ in the sum is $\langle \mathcal{P}_\lambda f, f \rangle = \|\mathcal{P}_\lambda f\|^2$, where \mathcal{P}_λ is the orthogonal spectral projector associated with the eigenvalue λ , and $\|\cdot\| = \sqrt{\langle \cdot, \cdot \rangle}$ is the norm on \mathcal{H} . The continuous part of μ_f consists of an absolutely continuous¹ part with Radon–Nikodym derivative $\rho_f \in L^1(\mathbb{R})$ and a singular continuous component $\mu_f^{(\text{sc})}$. Without loss of generality, we assume throughout that $\|f\| = 1$, which ensures that μ_f is a probability measure.

Computing μ_f is important in many applications, and can be considered an infinite-dimensional analogue of computing eigenvectors. We aim to evaluate smoothed approximations of μ_f . We compute a smooth function μ_f^ϵ , with smoothing parameter $\epsilon > 0$, that converges weakly to μ_f [15, Ch. 1]. That is,

$$\int_{\mathbb{R}} \phi(y) \mu_f^\epsilon(y) dy \rightarrow \int_{\mathbb{R}} \phi(y) d\mu_f(y), \quad \text{as} \quad \epsilon \downarrow 0, \quad (4)$$

for any bounded, continuous function ϕ .

3 Algorithmic framework for SpecSolve

Our key ingredient is the resolvent $(\mathcal{L} - z)^{-1} = \int_{\Lambda(\mathcal{L})} (\lambda - z)^{-1} d\mathcal{E}(\lambda)$ for $z \notin \Lambda(\mathcal{L})$. Stone's formula [16] links the resolvent to convolution with the Poisson kernel:

$$\mu_f^\epsilon(x) = \frac{-1}{\pi} \text{Im} \left(\langle (\mathcal{L} - (x - \epsilon i))^{-1} f, f \rangle \right) = \int_{\mathbb{R}} \frac{\epsilon \pi^{-1}}{(x - \lambda)^2 + \epsilon^2} d\mu_f(\lambda). \quad (5)$$

As $\epsilon \downarrow 0$, this approximation converges weakly to μ_f . To compute $(\mathcal{L} - (x - \epsilon i))^{-1} f$ we must somehow discretize the operator. However, for a given discretization size,

¹ We take ‘‘absolutely continuous’’ to be with respect to the Lebesgue measure.

Algorithm 1 A computational framework for evaluating an approximate spectral measure of an operator \mathcal{L} at $x_0 \in \mathbb{R}$ with respect to a vector $f \in \mathcal{H}$.

Input: $\mathcal{L}, f \in \mathcal{H}, x_0 \in \mathbb{R}, a_1, \dots, a_m \in \{z \in \mathbb{C} : \text{Im}(z) > 0\}$, and $\epsilon > 0$.

1: Solve the Vandermonde system (6) for the residues $\alpha_1, \dots, \alpha_m \in \mathbb{C}$.

2: Solve $(\mathcal{L} - (x_0 - \epsilon a_j))u_j^\epsilon = f$ for $1 \leq j \leq m$.

3: Compute $\mu_f^\epsilon(x_0) = \frac{-1}{\pi} \text{Im} \left(\sum_{j=1}^m \alpha_j \langle u_j^\epsilon, f \rangle \right)$.

Output: The approximate spectral measure $\mu_f^\epsilon(x_0)$.

if ϵ is too small, the approximation via (5) becomes unstable [12, Section 4.3] due to the discrete spectrum of the discretization. We must adaptively increase the discretization/truncation size as $\epsilon \downarrow 0$ and there is an increased computational cost for smaller ϵ . Therefore, replacing the Poisson kernel with higher-order rational kernels is advantageous. These kernels have better convergence rates as $\epsilon \downarrow 0$, allowing a larger ϵ to be used for a given accuracy, and thus a lower computational burden.

Let $\{a_j\}_{j=1}^m$ be distinct points in the upper half plane and suppose that the constants $\{\alpha_j\}_{j=1}^m$ satisfy the following (transposed) Vandermonde system:

$$\begin{pmatrix} 1 & \dots & 1 \\ a_1 & \dots & a_m \\ \vdots & \ddots & \vdots \\ a_1^{m-1} & \dots & a_m^{m-1} \end{pmatrix} \begin{pmatrix} \alpha_1 \\ \alpha_2 \\ \vdots \\ \alpha_m \end{pmatrix} = \begin{pmatrix} 1 \\ 0 \\ \vdots \\ 0 \end{pmatrix}. \quad (6)$$

Then the kernel

$$K(x) = \frac{1}{2\pi i} \sum_{j=1}^m \frac{\alpha_j}{x - a_j} - \frac{1}{2\pi i} \sum_{j=1}^m \frac{\overline{\alpha_j}}{x - \overline{a_j}} \quad \text{with } K_\epsilon(x) = \epsilon^{-1} K(x\epsilon^{-1})$$

is an m th order kernel, and we have the following generalization of Stone's formula

$$\mu_f^\epsilon(x) = [K_\epsilon * \mu_f](x) = \frac{-1}{\pi} \sum_{j=1}^m \text{Im} \left(\alpha_j \langle (\mathcal{L} - (x - \epsilon a_j))^{-1} f, f \rangle \right). \quad (7)$$

This provides $O(\epsilon^m \log(\epsilon^{-1}))$ convergence in (4) if ϕ is sufficiently regular, and similar rates for $\mu_f^\epsilon(x) \rightarrow \rho_f(x)$ if μ_f is sufficiently regular near x [12].

We consider the choice $a_j = 2j/(m+1) - 1 + i$ and the framework for evaluating μ_f^ϵ is summarized in Algorithm 1. This algorithm forms the foundation of SpecSolve [13] and can be performed in parallel for several x_0 . We compute an accurate value of μ_f^ϵ provided that the resolvent is applied with sufficient accuracy. For an efficient adaptive implementation, SpecSolve constructs a fixed discretization, solves linear systems at each required complex shift, and checks the approximation error at each shift. If further accuracy is needed at a subset of the shifts, then the discretization size is doubled, applied at these shifts, and the error is recomputed. This process is repeated until the resolvent is computed accurately at all shifts.

4 Singular integro-differential operators

Singular integral operators of Cauchy type play a pivotal role in the classical theory of PDEs and their spectral properties [17]. They appear in a wide range of physical models, along with their integro-differential and nonlinear counterparts [18].

Consider the self-adjoint singular integral operator \mathcal{L} in (1) with $G(x, y) = \overline{G(y, x)}$, and $a(x)$ real, continuously differentiable, and bounded. To compute spectral measures of \mathcal{L} in the SpecSolve framework, we must compute inner products between functions in $L^2(\mathbb{R})$ and solve linear equations with a complex shift z , e.g.,

$$(a(x) - z)u(x) + \frac{1}{\pi i} \int_{\mathbb{R}} \frac{G(x, y)}{y - x} u(y) dy = f(x). \quad (8)$$

We discretize $L^2(\mathbb{R})$ with the orthogonal rational basis functions $\rho_n(x) = \frac{1}{\sqrt{\pi}} \frac{(1+ix)^n}{(1-ix)^{n+1}}$, for $n \in \mathbb{Z}$. These functions have excellent approximation properties, are associated with banded differentiation and multiplication matrices, and expansion coefficients can be computed from function samples in quasi-linear time with the FFT [19]. Moreover, they diagonalize the Hilbert transform [20] and lead to banded discretizations of (8) when $G(x, y)$ is sufficiently smooth and of low numerical rank [21].

Both the multiplicative and integral components of \mathcal{L} can contribute continuous spectrum. When $G(x, y) = k(x)k(y)$ is a rank one kernel with $k(x) > 0$, the spectrum fills the interval $[\min |a(x) - k(x)|, \max |a(x) + k(x)|]$ [22]. Figure 1 (left) shows the spectral measures μ_f of \mathcal{L} , with $f(x) = \sqrt{2/\pi}(1-x^2)^{-1}$, $k(x) = e^{-x^2}$, and $a_{\pm}(x) = \pm 2/(1+x^2)^2$. The dashed grey lines highlight the support of the measures in the expected interval. We can also tackle singular integro-differential operators. Figure 1 (right) compares the spectral measures of $-d^2/dx^2$ and $-d^2/dx^2 + (1/\pi i) \int_{\mathbb{R}} (y-x)^{-1} dy$ with respect to f . Both the second derivative and the singular integral are diagonalized by the Fourier transform, and the spectral measures can be computed analytically (dashed lines). The integral perturbation breaks the symmetry between positive and negative Fourier modes, which effectively splits the spectral measure of $-d^2/dx^2$ into two duplicate peaks of half height at ± 1 .

The SpecSolve framework can also compute spectral projections $\mathcal{E}([a, b])$ associated with the projection-valued measure by omitting the inner product step in Algorithm 1 and applying endpoint corrections [23]. Figure 2 displays a scalar spectral measure and spectral projection for the partial integro-differential operator

$$-\Delta u + v(x, y)u + \frac{1}{\pi i} \int_{\mathbb{R}} \frac{\exp(-x^2 - y^2)}{y - x} u(\cdot, y) dy, \quad \mathcal{H} = L^2(\mathbb{R} \times [-1, 1]), \quad (9)$$

and the function $f(x, y) = (1+x)(1+x^2)^{-1} \cos(\pi y/2)/\sqrt{\pi}$. The potential function is $v(x, y)$ is also plotted in fig. 2. The operator is discretized with a tensor product basis of the rational orthogonal functions $\{\rho_n\}$ and ultraspherical polynomials [24], resulting in a sparse and banded discretization (we use basis reordering to reduce the bandwidth). In fig. 2, narrow peaks in the scalar measure reveal scattering resonances of the partial integro-differential operator and the associated spectral projections uncover wave-packet modes that are highly concentrated within the potential well.

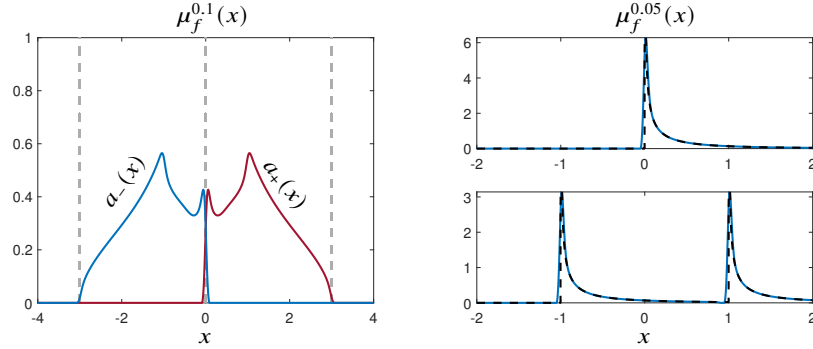


Fig. 1 Left: The smoothed spectral measures, $\mu_f^{0.1}$, computed with a 4th order kernel are supported on the intervals $[\min |a(x) - k(x)|, \max |a(x) + k(x)|]$. Right: The smoothed spectral measures, $\mu_f^{0.05}$, computed with a 4th order kernel for $-d^2/dx^2$ (top) and $-d^2/dx^2 + (1/\pi i) \int_{\mathbb{R}} (y-x)^{-1} dy$ (bottom) are compared with analytical solutions (dashed lines).

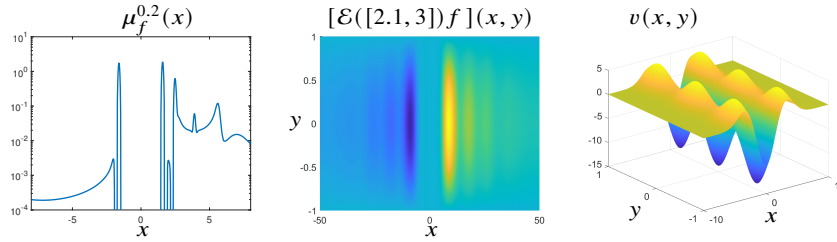


Fig. 2 Left: The smoothed spectral measure, $\mu_f^{0.2}$, of the partial integro-differential operator in (9) computed with a 6th order kernel. Middle: Spectral projection $\mathcal{E}([2.1, 3])f$ of $f(x, y) = (1+x)(1+x^2)^{-1} \cos(\pi y/2)/\sqrt{\pi}$ associated with the third resonance peak from the left in the plot of $\mu_f^{0.2}$. Right: The potential energy landscape $v(x, y)$ for the operator in (9).

5 Linear operator pencils

For matrices $A, B \in \mathbb{C}^n$, the classical generalized eigenvalue problem is the problem of finding $v \in \mathbb{C}^n \setminus \{0\}$ and $\lambda \in \mathbb{C}$ such that $Av = \lambda Bv$. For example, this problem arises in finite element discretizations of eigenproblems for elliptic partial differential operators, where A corresponds to the “stiffness matrix” and B corresponds to the “mass matrix” [25]. Another example is linearization methods for non-linear eigenvalue problems [26]. For many applications, A and B are finite approximations of (possibly unbounded) operators \mathcal{A} and \mathcal{B} acting on a separable Hilbert space. We consider the case that \mathcal{A} and \mathcal{B} are both self-adjoint and that \mathcal{B} is positive and invertible. We study the generalized spectral problem through the operator formally defined as $\mathcal{L} = \mathcal{B}^{-1}\mathcal{A}$.

5.1 Recovering a self-adjoint operator

It is well-known that $\mathcal{D}(\mathcal{B}^{1/2})$ is complete with respect to the norm $\|f\|_{\mathcal{B}} := \langle \mathcal{B}^{1/2}f, \mathcal{B}^{1/2}f \rangle$ [27, Theorem 4.4.2]. We denote the induced Hilbert space by $\mathcal{H}_{\mathcal{B}}$. The operator $\mathcal{B}^{-1}\mathcal{A}$ with domain $\mathcal{D}(\mathcal{A}) \cap \mathcal{D}(\mathcal{B}^{1/2})$ is symmetric in $\mathcal{H}_{\mathcal{B}}$.² However, to apply the spectral theorem, we need a self-adjoint operator. We assume that $\mathcal{D}(\mathcal{A}) \cap \mathcal{D}(\mathcal{B}^{1/2})$ is a dense subspace of the Hilbert space $\mathcal{H}_{\mathcal{B}}$. Since $\mathcal{B}^{-1}\mathcal{A}$ is symmetric in $\mathcal{H}_{\mathcal{B}}$, it is closable. We define the symmetric closed operator

$$\mathcal{L} = \overline{\mathcal{B}^{-1}\mathcal{A}|_{\mathcal{D}(\mathcal{A}) \cap \mathcal{D}(\mathcal{B}^{1/2})}}, \quad (10)$$

where the closure is performed with respect to $\mathcal{H}_{\mathcal{B}}$. This allows us to perform *numerical computations* with \mathcal{L} by restricting to the subspace $\mathcal{D}(\mathcal{A}) \cap \mathcal{D}(\mathcal{B}^{1/2})$. To do this, we consider the inner product space $\{f : f \in \mathcal{H}\}$ with inner product $\langle f, g \rangle_{\mathcal{B}^{-1}} = \langle \mathcal{B}^{-1/2}f, \mathcal{B}^{-1/2}g \rangle$. We take the completion of this space, $\mathcal{H}_{\mathcal{B}^{-1}}$. $\mathcal{D}(\mathcal{B})$ is dense in $\mathcal{H}_{\mathcal{B}}$ and hence \mathcal{B} can be extended to an invertible isometry from $\mathcal{H}_{\mathcal{B}}$ to $\mathcal{H}_{\mathcal{B}^{-1}}$, and $\mathcal{H}_{\mathcal{B}^{-1}}$ can be identified with the dual of $\mathcal{H}_{\mathcal{B}}$. We assume that $\mathcal{A}|_{\mathcal{D}(\mathcal{A}) \cap \mathcal{D}(\mathcal{B}^{1/2})} : \mathcal{H}_{\mathcal{B}} \rightarrow \mathcal{H}_{\mathcal{B}^{-1}}$ is closable, with closure denoted by $\mathcal{A}_{\mathcal{B}}$. We can now define

$$\begin{aligned} \mathcal{T}(z) : \mathcal{D}(\mathcal{A}_{\mathcal{B}}) &\rightarrow \mathcal{H}_{\mathcal{B}^{-1}}, & f &\mapsto (\mathcal{A}_{\mathcal{B}} - z\mathcal{B})f, \\ \Lambda(\mathcal{A}, \mathcal{B}) &= \{z \in \mathbb{C} : \mathcal{T}(z) \text{ does not have bounded inverse}\}. \end{aligned} \quad (11)$$

Proposition 1 *For any $z \in \mathbb{C}$, $\mathcal{D}(\mathcal{T}(z)) = \mathcal{D}(\mathcal{L})$ and $\mathcal{T}(z) = \mathcal{B}(\mathcal{L} - z)$. Moreover, $\Lambda(\mathcal{A}, \mathcal{B}) = \Lambda(\mathcal{L})$ and if $z \in \mathbb{C} \setminus \Lambda(\mathcal{L})$, then $(\mathcal{L} - z)^{-1} = \mathcal{T}(z)^{-1}\mathcal{B}$.*

Proof Let $z \in \mathbb{C}$ and $f \in \mathcal{D}(\mathcal{L})$. Then there exists $f_n \in \mathcal{D}(\mathcal{A}) \cap \mathcal{D}(\mathcal{B}^{1/2})$ such that $\lim_{n \rightarrow \infty} f_n = f$ (in $\mathcal{H}_{\mathcal{B}}$) and $\lim_{n \rightarrow \infty} (\mathcal{L} - z)f_n = (\mathcal{L} - z)f$ (in $\mathcal{H}_{\mathcal{B}}$). Since $\|\mathcal{T}(z)f_n - \mathcal{T}(z)f_m\|_{\mathcal{B}^{-1}} = \|(\mathcal{L} - z)f_n - (\mathcal{L} - z)f_m\|_{\mathcal{B}}$, it follows that $\{\mathcal{T}(z)f_n\}$ is Cauchy in $\mathcal{H}_{\mathcal{B}^{-1}}$ and hence converges to some $g \in \mathcal{H}_{\mathcal{B}^{-1}}$. Since $\mathcal{T}(z)$ is closed, $f \in \mathcal{D}(\mathcal{T}(z))$ and $\mathcal{T}(z)f = g$. Moreover, $\|(\mathcal{L} - z)f_n - \mathcal{B}^{-1}g\|_{\mathcal{B}} = \|\mathcal{T}(z)f_n - g\|_{\mathcal{B}^{-1}}$ converges to zero. Since \mathcal{L} is closed, $(\mathcal{L} - z)f = \mathcal{B}^{-1}g$ and hence that $\mathcal{B}(\mathcal{L} - z)f = \mathcal{T}(z)f$. A similar argument shows that $\mathcal{D}(\mathcal{T}(z)) \subset \mathcal{D}(\mathcal{L})$. Hence, $\mathcal{D}(\mathcal{T}(z)) = \mathcal{D}(\mathcal{L})$ and $\mathcal{T}(z) = \mathcal{B}(\mathcal{L} - z)$. The proposition follows since $\mathcal{B} : \mathcal{H}_{\mathcal{B}} \rightarrow \mathcal{H}_{\mathcal{B}^{-1}}$ is an isometry. \square

The following theorem that gives sufficient conditions for \mathcal{L} to be self-adjoint. Common examples of these conditions include when \mathcal{A} and \mathcal{B} are suitable elliptic PDEs of the same differentiation order (see condition (C1)), \mathcal{A} is bounded (see condition (C2)), and \mathcal{B} is a suitable weight function (see condition (C3))

Theorem 1 *Consider the operators \mathcal{A} , \mathcal{B} and \mathcal{L} above. Suppose that any of the following conditions hold:*

(C1) *There exist constants $a, b > 0$ such that for any $f \in \mathcal{D}(\mathcal{A}) \cap \mathcal{D}(\mathcal{B}^{1/2})$*

$$\|\mathcal{B}^{-1/2}\mathcal{A}f\| \leq a\|f\| + b\|\mathcal{B}^{1/2}f\|. \quad (12)$$

² Suppose that $f, g \in \mathcal{D}(\mathcal{A}) \cap \mathcal{D}(\mathcal{B}^{1/2})$. Then $\langle \mathcal{B}^{1/2}(\mathcal{B}^{-1}\mathcal{A})g, \mathcal{B}^{1/2}f \rangle = \langle \mathcal{B}^{-1/2}\mathcal{A}g, \mathcal{B}^{1/2}f \rangle = \langle \mathcal{A}g, f \rangle$. The first equality follows since $\mathcal{B}^{-1}\mathcal{A}g \in \mathcal{D}(\mathcal{B}^{1/2})$, whereas the second follows since $\mathcal{B}^{-1/2}$ is a bounded self-adjoint operator on \mathcal{H} . Similarly, we have that $\langle \mathcal{B}^{1/2}g, \mathcal{B}^{1/2}(\mathcal{B}^{-1}\mathcal{A})f \rangle = \langle g, \mathcal{A}f \rangle$.

(C2) \mathcal{A} is a relatively bounded perturbation of \mathcal{B} , meaning that $\mathcal{D}(\mathcal{B}) \subset \mathcal{D}(\mathcal{A})$ and there exist constants $a, b > 0$ such that for any $f \in \mathcal{D}(\mathcal{B})$

$$\|\mathcal{A}f\| \leq a\|f\| + b\|\mathcal{B}f\|. \quad (13)$$

(C3) $\text{Sp}(\mathcal{A}) \neq \mathbb{R}$ and \mathcal{B} is a relatively bounded perturbation of \mathcal{A} , meaning that $\mathcal{D}(\mathcal{A}) \subset \mathcal{D}(\mathcal{B})$ and there exist constants $a, b > 0$ such that for any $f \in \mathcal{D}(\mathcal{A})$

$$\|\mathcal{B}f\| \leq a\|f\| + b\|\mathcal{A}f\|. \quad (14)$$

Then \mathcal{L} is self-adjoint on $\mathcal{H}_{\mathcal{B}}$. Moreover, when (C1) holds, \mathcal{L} is bounded.

Proof Suppose first that (C1) holds. Since $\mathcal{B}^{1/2}$ is strictly positive, (12) implies that there exists a positive constant c such that $\|\mathcal{B}^{-1/2}\mathcal{A}f\| \leq c\|\mathcal{B}^{1/2}f\|$ for any $f \in \mathcal{D}(\mathcal{A}) \cap \mathcal{D}(\mathcal{B}^{1/2})$. This is equivalent to boundedness of $\mathcal{B}^{-1}\mathcal{A}|_{\mathcal{D}(\mathcal{A}) \cap \mathcal{D}(\mathcal{B}^{1/2})}$ in the Hilbert space $\mathcal{H}_{\mathcal{B}}$, and hence \mathcal{L} is bounded and self-adjoint on $\mathcal{H}_{\mathcal{B}}$.

For (C2) or (C2), we claim that it is enough to show that there exists some $\gamma > 0$ and $\kappa \in \mathbb{R}$ such that the operators

$$T_{\pm} = \mathcal{A} + \kappa I \pm i\gamma\mathcal{B}, \quad \mathcal{D}(T_{\pm}) = \mathcal{D}(\mathcal{A}) \cap \mathcal{D}(\mathcal{B}) \quad (15)$$

are closable (in \mathcal{H}), and that their closures, denoted \overline{T}_{\pm} , are invertible (in \mathcal{H}). To see this, suppose that these conditions hold. Let $g \in \mathcal{D}(\mathcal{B})$ and set $f^{\pm} = \overline{T}_{\pm}^{-1}\mathcal{B}g$. Then, by definition of the closure, there exists $f_n^{\pm} \in \mathcal{D}(\mathcal{A}) \cap \mathcal{D}(\mathcal{B}) \subset \mathcal{D}(\mathcal{A}) \cap \mathcal{D}(\mathcal{B}^{1/2})$ such that $f_n^{\pm} \rightarrow f^{\pm}$ and $T_{\pm}f_n^{\pm} \rightarrow \mathcal{B}g$ as $n \rightarrow \infty$ (with convergence in \mathcal{H}). Thus, $\|\mathcal{B}^{-1}(\mathcal{A} + \kappa I)f_n^{\pm} \pm i\gamma f_n^{\pm} - g\|_{\mathcal{B}} = \|\mathcal{B}^{-1/2}(T_{\pm}f_n^{\pm} - \mathcal{B}g)\| \rightarrow 0$ as $n \rightarrow \infty$. Since $\mathcal{D}(\mathcal{B})$ is dense in $\mathcal{H}_{\mathcal{B}}$, it follows that the ranges of $\gamma^{-1}\mathcal{B}^{-1}(\mathcal{A} + \kappa I) \pm iI$ are also dense in $\mathcal{H}_{\mathcal{B}}$. It follows that $\gamma^{-1}\mathcal{B}^{-1}(\mathcal{A} + \kappa I)$ is essentially self-adjoint in $\mathcal{H}_{\mathcal{B}}$ [14, p. 257], and hence so is $\mathcal{B}^{-1}\mathcal{A}$. This proves the claim.

Now suppose that (C2) holds. Since \mathcal{B} is strictly positive, (13) implies that there exists a positive constant $c < 1$ and $\gamma > 0$ such that $\|\mathcal{A}f\| \leq c\|\gamma\mathcal{B}f\|$ for any $f \in \mathcal{D}(\mathcal{B}) \subset \mathcal{D}(\mathcal{A})$. Hence \mathcal{A} is a relatively bounded perturbation of $i\gamma\mathcal{B}$, with $i\gamma\mathcal{B}$ -bound less than 1. Stability of bounded invertibility [28, Theorem IV.4.1.16] implies that T_{\pm} in (15) (with $\kappa = 0$) are closed and invertible (in \mathcal{H}).

Finally, suppose that (C3) holds. Choose $\kappa \in \mathbb{R}$ with $-\kappa \notin \text{Sp}(\mathcal{A})$ so that $\mathcal{A} + \kappa I$ is invertible, and set $C = \mathcal{A} + \kappa I$. For any $f \in \mathcal{D}(\mathcal{A})$ and $\gamma > 0$, (14) implies that

$$\|\gamma\mathcal{B}f\| \leq \gamma(a + |\kappa|)\|f\| + \gamma b\|Cf\|. \quad (16)$$

Choose $\gamma > 0$ so that $\gamma(a + |\kappa|)\|C^{-1}\| + \gamma b < 1$. The stability of bounded invertibility [28, Theorem IV.4.1.16] and (16) imply that T_{\pm} are closed and invertible. \square

5.2 Framework for generalized spectral measures

To extend SpecSolve to the above pencil problem, we simply apply (7) with the operator \mathcal{L} defined in (10) and the Hilbert space $\mathcal{H}_{\mathcal{B}}$. We suppose for simplicity that $f \in \mathcal{D}(\mathcal{B})$. Using proposition 1 and (7) and the self-adjointness of $\mathcal{B}^{1/2}$, we have

Algorithm 2 A computational framework for evaluating an approximate spectral measure of an operator \mathcal{L} in (10) corresponding to the pencil $\mathcal{A} - \lambda\mathcal{B}$ at $x_0 \in \mathbb{R}$ with respect to a vector $f \in \mathcal{D}(\mathcal{B})$.

Input: $\mathcal{A}, \mathcal{B}, f \in \mathcal{D}(\mathcal{B}), x_0 \in \mathbb{R}, a_1, \dots, a_m \in \{z \in \mathbb{C} : \text{Im}(z) > 0\}$, and $\epsilon > 0$.

- 1: Compute $g = \mathcal{B}f$.
- 2: Solve the Vandermonde system (6) for the residues $\alpha_1, \dots, \alpha_m \in \mathbb{C}$.
- 3: Solve $(\mathcal{A} - (x_0 - \epsilon a_j)\mathcal{B})\mu_j^\epsilon = g$ for $1 \leq j \leq m$.
- 4: Compute $\mu_f^\epsilon(x_0) = \frac{-1}{\pi} \text{Im} \left(\sum_{j=1}^m \alpha_j \langle u_j^\epsilon, g \rangle \right)$.

Output: The approximate spectral measure $\mu_f^\epsilon(x_0)$.

$$\begin{aligned} \mu_f^\epsilon(x) &= [K_\epsilon * \mu_f](x) = \frac{-1}{\pi} \sum_{j=1}^m \text{Im} \left(\alpha_j \langle (\mathcal{B}^{1/2} \mathcal{T}(x - \epsilon a_j)^{-1} \mathcal{B}f, \mathcal{B}^{1/2} f) \rangle \right) \\ &= \frac{-1}{\pi} \sum_{j=1}^m \text{Im} \left(\alpha_j \langle (\mathcal{T}(x - \epsilon a_j)^{-1} \mathcal{B}f, \mathcal{B}f) \rangle \right), \end{aligned} \quad (17)$$

where we use that $\mathcal{B}^{1/2}$ is self-adjoint in the second line and $\langle \cdot, \cdot \rangle$ denotes the inner product on \mathcal{H} . This leads to Algorithm 2, which generalizes Algorithm 1. To apply Algorithm 2, we only need to compute approximations of $g = \mathcal{B}f$, solve the systems $(\mathcal{A} - (x_0 - \epsilon a_j)\mathcal{B})u_j^\epsilon = g$, and then compute inner products. We approximate u_j^ϵ using spectral methods and compute inner products using quadrature.

5.3 Examples

We now present two examples, using Fourier spectral methods and a spectral element method, respectively. Both examples fall into the setup of Theorem 1.

Pseudo-differential operators and internal waves: Spectral properties of 0th order pseudo-differential operators arise naturally in fluid mechanics [29] and pseudoparabolic equations [30]. See [31, 32] for the study of internal waves and [33, 34] for connections with scattering resonances. As a simple example, we consider

$$\mathcal{A} = -i(1 + \cos(x)/2)\partial_y, \quad \mathcal{B} = (1 - \partial_y^2)^{1/2}, \quad x, y \in [-\pi, \pi]_{\text{per}},$$

where the initial Hilbert space is $\mathcal{H} = L^2([-\pi, \pi]_{\text{per}}^2)$. To solve the linear systems in Algorithm 2, we use the standard tensor product Fourier basis.

Figure 3 (left) shows the smoothed spectral measures computed using $\epsilon = 0.01$, and the first and sixth-order kernels for $f(x, y) = C \exp(\sin(x + y))/(2 + \cos(y))$, where C is a normalization constant so that μ_f is a probability measure. The spectral measure has an absolutely continuous component (with piecewise continuous Radon–Nikodym derivative), and an eigenvalue at 0. The higher order kernel ($m = 6$) provides a better localization of the singular part of the spectral measure at 0, and also a better resolution of jumps in the Radon–Nikodym derivative (see zoomed-in

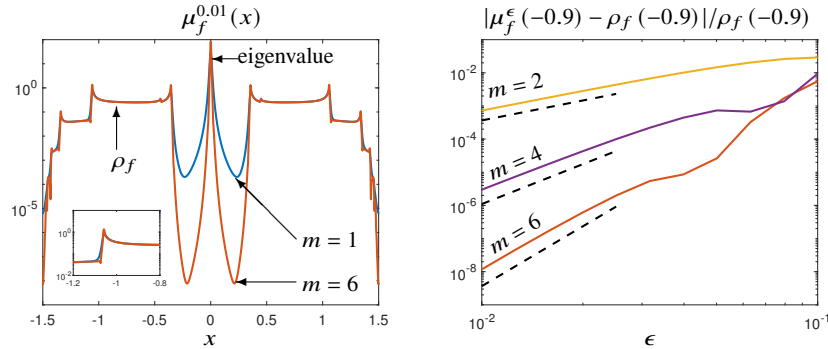


Fig. 3 Left: Smoothed spectral measures, $\mu_f^{0.01}$, computed using the 1st and 6th order kernels. The zoomed-in section shows better resolution of jump discontinuities in ρ_f for larger m . Right: Relative pointwise convergence to ρ_f and expected rates shown as dashed black lines.

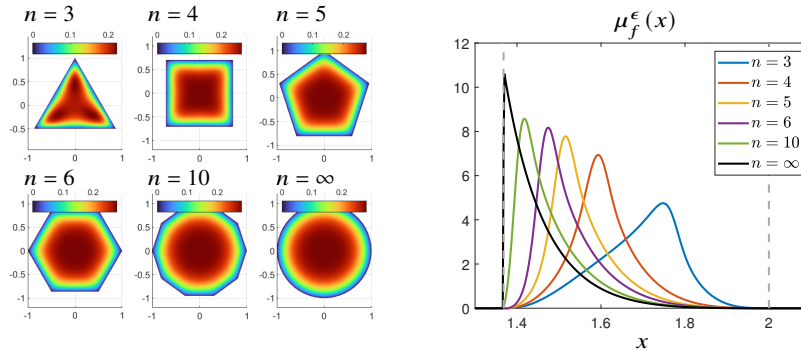


Fig. 4 Left: Functions f for different n . Right: Smoothed spectral measures, μ_f^ϵ , for different n -gons computed using the 6th order kernel. For $n < \infty$ we use $\epsilon = 0.05$ and for the circle we use $\epsilon = 0.001$. The dashed vertical lines are the endpoints of the spectrum.

section). Figure 3 (right) shows the pointwise convergence to the Radon–Nikodym derivative and the expected rates of convergence for $m = 2, 4$ and 6 .

Elliptic differential operator preconditioners: A common use of \mathcal{L} in (10) is preconditioning, where \mathcal{B} is a preconditioner of \mathcal{A} [35]. For example, sometimes one can prove mesh-independent bounds on condition numbers for methods such as finite elements [36], which are useful for applying Krylov space methods. The papers [37, 38] discuss the spectrum of \mathcal{L} in this context. The spectral measure of \mathcal{L} and its discretizations determine the behavior of Krylov subspace methods. See [37, Section 2] for an instructive example for which the spectrum is not enough.

We follow [39] and consider a bounded Lipschitz domain $\Omega \subset \mathbb{R}^2$. We take

$$\mathcal{A}u = -\nabla \cdot [(1 + \exp(-x^2 - y^2))\nabla u], \quad \mathcal{B}u = -\nabla^2 u,$$

both with zero Dirichlet boundary conditions. The spectrum of \mathcal{L} is the interval [39] $\Lambda(\mathcal{L}) = [\inf_{(x,y) \in \Omega} 1 + \exp(-x^2 - y^2), \sup_{(x,y) \in \Omega} 1 + \exp(-x^2 - y^2)]$, but the spectral

measure is unknown. To solve the linear systems in Algorithm 2, we use the (hp -adaptive and sparse) ultraspherical spectral element method [40].

We take Ω to be a regular n -gon and set $f = C(\Omega)\mathcal{B}^{-1}g$, where $g(x, y) = x^2 + y^2$ and $C(\Omega)$ are normalization constants so that each μ_f is a probability measure. Figure 4 (left) shows these f and fig. 4 (right) shows the smoothed spectral measures. The endpoints of the spectrum are shown as vertical dashed lines. The measures appear to be absolutely continuous and converge to the corresponding measure for the disk ($n = \infty$) as n gets larger. To deal with the disk, we use separation of variables and solve the resulting radial ODEs using the ultraspherical spectral method [24].

Acknowledgements MJC is supported by a Research Fellowship at Trinity College, Cambridge, and a Fondation Sciences Mathématiques de Paris Postdoctoral Fellowship at École Normale Supérieure. We thank Alex Townsend for pointing out that separation of variables efficiently deals with the $n = \infty$ case in fig. 4 and for reading a draft version of the article. We thank Zdenek Strakos for discussions on the preconditioner example and for reading a draft version of the article.

References

1. Kallianpur, G. and Mandrekar, V.: Spectral theory of stationary H-valued processes. *J. Multivar. Anal.* **1**, 1–16 (1971)
2. Girardin, V. and Senoussi, R.: Semigroup stationary processes and spectral representation. *Bernoulli* **9**, 857–876 (2003)
3. Rosenblatt, M.: Stochastic curve estimation. NSF-CBMS Regional Conference Series in Probability and Statistics **3**, (1991)
4. Efros, V. D., Leidemann, W., Orlandini, G. and Barnea, N.: The Lorentz integral transform (LIT) method and its applications to perturbation-induced reactions. *J. Phys. G*, **34**, (2007)
5. Efros, V. D., Leidemann, W. and Orlandini, G.: Response functions from integral transforms with a Lorentz kernel. *Phys. Lett. B*, **338**, 130–133 (1994)
6. Haydock, R., Heine, V. and Kelly, M. J.: Electronic structure based on the local atomic environment for tight-binding bands. *J. Phys. C: Solid State Phys.* **5**, (1972)
7. Lin, L., Saad, Y. and Yang, C.: Approximating spectral densities of large matrices. *SIAM Rev.*, **58**, 34–65 (2016)
8. Wilkening, J. and Cerfon, A.: A spectral transform method for singular Sturm–Liouville problems with applications to energy diffusion in plasma physics. *SIAM J. Appl. Math.*, **75**, 350–392 (2015)
9. Killip, R. and Simon, B.: Sum rules for Jacobi matrices and their applications to spectral theory. *Ann. Math.*, **158**, 253–321 (2003)
10. Dombrowski, J. and Nevai, P.: Orthogonal polynomials, measures and recurrence relations. *SIAM J. Math. Anal.*, **17**, 752–759 (1986)
11. Trogdon, T., Olver, S. and Deconinck, B.: Numerical inverse scattering for the Korteweg–de Vries and modified Korteweg–de Vries equations. *Phys. D: Nonlinear Phenom.*, **241**, 1003–1025 (2012)
12. Colbrook, M. J., Horning, A. and Townsend, A.: Computing spectral measures of self-adjoint operators. *SIAM Rev.*, **63** 489–524 (2021)
13. Colbrook, M. J. and Horning, A.: SpecSolve, <https://github.com/SpecSolve/SpecSolve>, (2020)
14. Reed, M. and Simon, B.: *Methods of Modern Mathematical Physics. I.* Academic Press, Inc., Harcourt Brace Jovanovich, New York, second edition (1980)

15. Billingsley, P.: *Convergence of Probability Measures*. John Wiley & Sons, second edition (1999)
16. Stone, M. H.: *Linear Transformations in Hilbert Space*. Amer. Math. Soc. Colloq. Pub. **15**, (1990)
17. Muskhelishvili, N. I. and Radok, J. R. M.: *Singular integral equations: boundary problems of function theory and their application to mathematical physics*. Noordhoff, Groningen (1953)
18. Cuminato, J. A., Fitt, A. D., and McKee, S.: A review of linear and nonlinear Cauchy singular integral and integro-differential equations arising in mechanics. *J. Integral Equ. Appl.* **163–207** (2007)
19. Iserles, A. and Webb, M.: A family of orthogonal rational functions and other orthogonal systems with a skew-Hermitian differentiation matrix. *J. Fourier Anal. Appl.* **26**, 1–28 (2020)
20. Weideman, J. A. C.: Computing the Hilbert transform on the real line. *Math. Comput.* **64**, 745–762 (1995)
21. Slevinsky, R. M., and Olver, S.: A fast and well-conditioned spectral method for singular integral equations. *J. Comput. Phys.* **332**, 290–315 (2017)
22. Koppelman, W.: On the spectral theory of singular integral operators. *Trans. Amer. Math. Soc.*, **97**, 35–63 (1960)
23. Colbrook, M. J., Horning, A., Thicke, K., and Watson, A. B.: Computing spectral properties of topological insulators without artificial truncation or supercell approximation. *arXiv:2112.03942* (2021)
24. Olver, S. and Townsend, A.: A fast and well-conditioned spectral method. *SIAM Rev.* **55**, 462–489 (2013)
25. Boffi, D.: Finite element approximation of eigenvalue problems. *Acta Numer.* **19**, 1–120 (2010)
26. Güttel, S. and Tisseur, F.: The nonlinear eigenvalue problem *Acta Numer.* **26**, 1–94 (2017)
27. Davies, E. B.: *Spectral Theory and Differential Operators*. Cambridge University Press (1996).
28. Kato, T.: *Perturbation Theory for Linear Operators*. Springer Science & Business Media (1976).
29. Ralston, J.: On stationary modes in inviscid rotating fluid. *J. Math. Anal. Appl.* **44**, 366–383 (1973)
30. Showalter, R. and Ting, T.: Pseudoparabolic partial differential equations. *SIAM J. Math. Anal.* **1**, 1–26 (1970)
31. Colin De Verdiere, Y. and Saint-Raymond, L.: Attractors for Two-Dimensional Waves with Homogeneous Hamiltonians of Degree 0. *Commun. Pure Appl. Math.* **73**, 421–462 (2020)
32. Colin De Verdiere, Y.: Spectral theory of pseudodifferential operators of degree 0 and an application to forced linear waves. *Analysis & PDE* **13**, 1521–1537 (2020)
33. Dyatlov, S., and Zworski, M.: Microlocal analysis of forced waves. *Pure and Applied Analysis* **1** 359–384 (2019)
34. Galkowski, J., and Zworski, M.: Viscosity limits for 0th order pseudodifferential operators. *Commun. Pure Appl. Math.*, to appear.
35. Málek, J. and Strakoš, Z.: Preconditioning and the Conjugate Gradient Method in the Context of Solving PDEs. *SIAM* (2014).
36. Mardal, K.-A. and Winther, R.: Preconditioning discretizations of systems of partial differential equations. *Numer. Linear Algebra Appl.* **18**, 1–40 (2011)
37. Gergelits, T. and Mardal, K.-A. and Nielsen, B. and Strakos, Z.: Laplacian preconditioning of elliptic PDEs: Localization of the eigenvalues of the discretized operator. *SIAM J. Numer. Anal.* **57**, 1369–1394 (2019)
38. Gergelits, T. and Nielsen, B. and Strakos, Z.: Generalized spectrum of second order differential operators. *SIAM J. Numer. Anal.* **58**, 2193–2211 (2020)
39. Gergelits, T., Nielsen, B. and Strakoš, Z.: Numerical approximation of the spectrum of self-adjoint operators and operator preconditioning. *arXiv:2103.00849* (2021)
40. Fortunato, D., Hale, N., and Townsend, A.: The ultraspherical spectral element method. *J. Comput. Phys.* **436** (2021)